This article has been accepted for publication in a future issue of this journal, but has not been fully edited. Content may change prior to final publication. Citation information: DOI 10.1109/TSTE.2018.2877106, IEEE Transactions on Sustainable Energy

Smart Wire Placement to Facilitate Large-Scale Wind Energy Integration: An Adaptive Robust Approach

Ahmad Nikoobakht, Jamshid Aghaei, *Senior Member, IEEE,* Taher Niknam, *Member, IEEE*, Miadreza Shafie-khah*, Senior Member, IEEE,* João P. S. Catalão*, Senior Member, IEEE*

***Abstract*—Enhanced utilization of the existing transmission grid is a cheaper and paramount way to have a high penetration of large-scale wind energy resources (WERs). Smart wire devices (SWDs) are a new technology to enhance the transfer capability through power flow control. The SWDs are distributed, cheap, self-governing smart assets of FACTS technologies, which can adjust the power flow in an interconnected transmission network. Accordingly, this paper presents a comprehensive three-stage robust SWD placement model, which minimizes the generation and investment costs while guaranteeing that the adaptive and secure robust solution is accustomed to cover the wind uncertainty interval. Since the proposed robust model is not solvable via an off-the-shelf optimization package and to reduce the computation burden of the solution process, an effective solution strategy is proposed to solve it. Detailed simulation results on the IEEE 24-bus system verify the effectiveness of the proposed robust SWD placement model.**

***Index Terms*—Smart wire devices, robust optimization and large-scale wind energy integration.**

I. Notation

A. Indices

$(\cdot)^u$	Related to uncertain variables.
g/w	Index for generating unit/wind farm.
n,m	Indices of buses.
k	Index of all transmission branches.
t	Index of time.
$\wedge$	Given variables/parameters.

B. Parameters

$P_g^{\max}$ / $P_g^{\min}$	Max/min. power generation of unit g.
D_{nt}	Load at bus n.
$\Delta r_{g,t}$	Up/down corrective action limit of unit g.
β_k^{max}	Maximum level of SWD compensation.
$P_{f,wt}$	Wind power forecast for wind farm w.
$\theta_n^{\max}$ / $\theta_n^{\min}$	Max/min of bus angle n.
$F_k^{\max}$	Max limit for power flow of line k.
η	Number of existing SWDs.
M	A given big number.

C. Variables

b_k	Susceptance of line k.
$\beta_{k,(\cdot)}^{(\cdot)}$	Compensation level of Susceptance of line k.
$\upsilon_{k,(\cdot)}$	Indicating the direction of power flow in line k.
z_k	Indicating the placement of SWD on line k.
$u_{g,(\cdot)}$	Unit status.
$\theta_{n,t}^{(\cdot)}$	Phase angle of bus n.
$P_{f,wt}$ / $P_{f,wt}^u$	Forecasted/ uncertain wind generation w.
$\overline{P}_{wt}$ / P_{wt}^u	Variation range of P_{wt}^u /worst-case realization.
$P_{gt}^{(\cdot)}$	Power generation of unit g.
$F_{k,(\cdot)}$ / $\Psi_{k,(\cdot)}$	Power flow on line k /with SWD.
$\Phi_{(\cdot)}, \vartheta_{(\cdot)}$	Slack variables.
$\Re^{worst}$	Worst-case realizations of subproblem II.
$\ell_{(\cdot)}$	Dual variable of constraint.
$\kappa_{(\cdot)}^{(\cdot)}$	Dual variables.

J.P.S. Catalão acknowledges the support by FEDER funds through COMPETE 2020 and by Portuguese funds through FCT, under Projects SAICT-PAC/0004/2015 - POCI-01-0145-FEDER-016434, POCI-01-0145-FEDER-006961, UID/EEA/50014/2013, UID/CEC/50021/2013, UID/EMS/00151/2013, and 02/SAICT/2017 - POCI-01-0145-FEDER-029803.

A. Nikoobakht is with the Higher Education Center of Eghlid, Eghlid, Iran-(email: a.nikoobakht@eghlid.ac.ir).

J. Aghaei and T. Niknam are with the Department of Electrical and Electronics Engineering, Shiraz University of Technology, Shiraz, Iran (e-mails: aghaei@sutech.ac.ir, niknam@sutech.ac.ir).

Miadreza Shafie-khah is with INESC TEC, Porto 4200-465, Portugal (e-mail: miadreza@gmail.com).

João P. S. Catalão is with INESC TEC and the Faculty of Engineering of the University of Porto, Porto 4200-465, Portugal, also with C-MAST, University of Beira Interior, Covilhã 6201-001, Portugal, and also with INESC-ID, Instituto Superior Técnico, University of Lisbon, Lisbon 1049-001, Portugal (e-mail: catalao@ubi.pt).

II. Introduction

Large-scale integration of wind energy resources (WERs) is expected to increase the variability and uncertainty in the power system. Variability and uncertainty are inherent characteristics of WERs resulting in technical and economic challenges for power system operators. In order to maintain the security of the system, a significant amount of wind generation resources may be curtailed. Also a large amount of ramping capacity is required to compensate for the uncertainty associated with wind energy generation in the unit commitment (UC) stage. Generally in a UC problem, conventional generating resources have sufficient ramping capability to cope with the variability and uncertainty of WERs. The effectively cope with the uncertainty and variability of the WERs would be achieved when the ramping capability of conventional generating resources coordinates with WERs variability and uncertainty. But, to cope with WER uncertainty and reduce wind energy spillage (WES), these ramping capabilities must be distributed throughout the transmission network with careful consideration of existing transmission constraints.

These ramping capabilities are difficult to distribute throughout the transmission network, as the transmission network is designed for conventional dispatchable CGRs rather than intermittent WERs. Insufficient transmission capacity in transmission network with bottlenecks are the most common reason to do not deliver a large amount of ramping capabilities throughout the transmission network and the involuntary WES. To enhance the transmission capacity and facilitate the wind WERs integration, three general approaches have been suggested: (i) adding energy storage systems (ESSs) to the system or using demand response program (DRP) to mitigate transmission congestion or enhance the transmission capacity and cope with WER uncertainty (or reduce WES) [1] and [2], (ii) construct new transmission lines [3] and (iii) improves the utilization of the existing transmission infrastructure by changing the impedance of the existing transmission line in network by employing variable-impedance flexible AC transmission system (FACTS) devices (VIT-FACTS), e.g., thyristor-controlled series compensators (TCSCs) and the newly manufactured Smart Wire devices (SWDs) [4], [5], [6] and [7].

The ESSs in *transmission networks*, including compressed air storage (CAS) [8] and pumped storage [1], can effectively maintain the power supply balance and mitigate the uncertainty of WERs. In [1], the pumped storage as a solution to store

This article has been accepted for publication in a future issue of this journal, but has not been fully edited. Content may change prior to final publication. Citation information: DOI 10.1109/TSTE.2018.2877106, IEEE Transactions on Sustainable Energy

energy is proposed and its effects on transmission congestion management, WES and other operational issues are studied. *This approach is very attractive once the cost of energy storage is reasonable.* Alike, the DRP in *transmission systems* can be utilized to accommodate the integration of WER and reduce involuntary WES *significantly* [2]. In [2], DRP has been implemented to cover transmission limit violations caused by WERs uncertainty. However, implementing these two approaches are limited in *transmission systems* by the high cost of ESSs and the lack of load flexibility (implementing the DRP in real-world for *transmission systems* is very difficult). On the other hand, building new transmission lines in order to reduce long-term wind curtailment is generally costly and may take a long time to be constructed. Thus, it is essential to make full use of the existing transmission network and harness the flexibilities of the transmission system, before building new lines. In this way, there are two technologists that could enhance the operational capacity of existing transmission lines, (i) TCSCs and (ii) SWDs [6], [7] and [9].

As mentioned above, in operation stage (or UC stage) transmission congestion in a power grid limits the generation output of WERs and increases WES. In the UC stage the power flow control capability introduced by TCSCs and SWDs, transmission bottlenecks can be avoided by shifting the power from the congested lines to the underutilized lines nearby. The TCSCs and SWDs have the potential to bring in additional available transfer capability to transmit more power from wind energy generating resources to meet the load. In addition, due to their fast operations, i.e., often within a few cycles of system frequency, TCSCs and SWDs can be dynamically adjusted to accommodate the uncertainty nature of WER [10]. While the allocation of TCSCs and SWDs is very expensive, its cost is small in comparison to installing ESSs. Despite the TCSC device can efficiently regulate active power flow, its usage is limited on account of its reliability and high costs [6] and [7]; although, the SWD, as an economic alternative, is capable of dealing with the existing concerns with the conventional series FACTS devices. For instance, in [7] the approximate price of SWD is about 105 $/kVAr in comparison with the cost of TCSC, i.e., 153 $/kVar [6]. The Georgia Tech has expanded the SWD technology to make a smart transmission line with the capability of regulating the power flow to shift the surplus power flow to lightly loaded lines in the grid [11]. Similarly, the SWD has been installed successfully on real networks such as the French transmission grid and Minnesota Power company RTE [11].

The SWD technology is a distributed solution, with a number of modules joined to the line conductor and separate operation of each smart wire module results in much more cost-efficiency and reliability with respect to the centralized FACTS devices [3] and [11]. Indeed, the SWDs have simple structure and functioning which can be installed in existing transmission lines, and they have the capability to increase transmission line impedance by injecting inductive reactance in series with the transmission line [12]. Therefore, they can control the power flow by changing the transmission line impedance to "push" power from high loaded lines into other lightly loaded lines of the transmission grid, i.e., deflect power flow to lightly loaded lines [9], [12] and [13]. Nowadays, increasing integration of stochastic WERs has made the SWD placement problem more complex. Indeed, ignoring uncertainty of WERs may result in unexpected insecure and costly results in the real-time operation [14]. Hence, stochastic approaches (SAs) and robust approach (RA) [15]–[16], [17] can be used to solve the optimal placement of SWDs under different uncertain situations resulting from wind uncertainty [14].

In the SA, generally, probability distributions function (PDF) of the uncertain inputs should be specified to generate scenarios, which is a challenging task in real-world utilization [15]. In contrast, the RA relies on the uncertainty interval of parameters rather than PDFs of uncertain variables [16]. Also, the SA method that needs to generate a high number of scenarios to cover much more uncertainty spectrum, may be resulted in infeasibility even for large optimal gaps. Nevertheless, the RA only relies on somehow the worst-case scenario of the uncertainty set which is a much more tractable optimization problem from the computational burden perspective [16]. There is no work in the reported technical literature that considers on an adaptive robust approach to the SWD (or VIT-FACTS) placement. In recent research works in the area of VIT-FACTS placement, mostly, the SA is adopted to deal with the uncertainties [14], [18], [13], [19] and [20]. The TCSC placement and operation problems considering SA has been tackled in [13] and [14].

The proposed model in this paper differs from the references [18], [13], [19] and [20] in three respects: 1) In comparison with [18], [13], [19] and [20], the proposed model is based on allocation of SWD. The SWD just with an increase of transmission line impedance can improve the transfer capability. 2) While stochastic programming is used in [18], [13] and [20], the proposed model in this paper is developed within an adaptive robust optimization framework considering wind uncertainty. When applying the stochastic approach, a large set of scenarios is required to ensure an accurate representation of the uncertainty involved, and this may cause computational intractability if large systems are considered. On the contrary, the robust approach describes the uncertainty using an uncertainty set, and hence, the problem maintains a moderate size. 3) Developing an accelerating and effective solution strategy based on combining the Benders' decomposition and a novel heuristic technique for pre-screen lines for the SWD allocation to solve the proposed problem through the wind uncertainty, which is not presented in [18], [13], [19] and [20]. Noted that to the best of our knowledge, only works by [14], [18], [13] and [20], try to develop the concept of using grid side flexibilities. Nonetheless, the robust operation and placement of SWD under wind uncertainty have not been addressed by the available researches in the area. Accordingly, the main aim of this work is to explore an adaptive robust optimization framework for concluding the optimal generation and investment costs while using the flexibility of SWD is permitted. Nevertheless, including the SWD and other series FACTS devices in the operation procedures will reveal some complexities in the system power flow model [19]. Indeed, originally, the proposed robust SWD placement with a linear objective function and the DC power flow is a mixed integer linear program (MILP); once the SWD is taken into consideration, the proposed model changes to a mixed integer nonlinear program (MINLP).

Dealing with the MINLP problem, considering the allowed timeframe, is out of the prevailing computational capabilities. Accordingly, the proposed MINLP formulation has been converted into a MILP-based robust SWD placement problem in this paper. Finally, note that the solution to the proposed robust formulation, as a min-max optimization problem, with the SWD placement, is hard to obtain without a proper approach.

Consequently, a fast-tracking solution approach is adopted here using the tri-level decomposition algorithm accompanying with a heuristic pre-screening procedure of all lines to choose limited candidates for installation of SWD.

All in all, as above mentioned, the paper aims to address the following questions: "*would different realizations of uncertainty of WERs affect the optimal placement of SWD*?" and "*would installation of the SWD, just with ability to increase line impedance, in transmission systems influence the utilization of wind energy and generation cost?*".

Considering the above addressed existing literature and identifying the state-of-art challenges, the novelties of this work are threefold:

(i) An adaptive *max-min* robust framework is explored for the SWD placement problem with wind uncertainty. The

This article has been accepted for publication in a future issue of this journal, but has not been fully edited. Content may change prior to final publication. Citation information: DOI 10.1109/TSTE.2018.2877106, IEEE Transactions on Sustainable Energy

proposed method discovers a robust solution which is immunized against different levels of wind power generation (WPG) uncertainty. As we know, there is no adaptive linear robust SWD placement formulation reported in the literature.

(ii) The proposed method based on the linear DC power flow model enables the harnessing grid side flexibility through SWD to enhance the WPG absorption under different realizations of uncertain WPGs.

(iii) A fast-tracking solution approach is developed which combines a tri-level decomposition algorithm and an innovative pre-screening procedure of lines to select the candidate lines for SWD placement.

III. Problem Statement

A. Assumptions

To have more clarifications, the main assumptions in the proposed modeling are as follows:

- Only wind energy uncertainty has been considered in the paper. The aim of this paper is to investigate the effect of SWD placement on wind uncertainty and vice versa. Consequently, demand uncertainty and equipment failures have not been considered in this paper. Nevertheless, it is straightforward to include the demand uncertainty or/and equipment failures in the proposed robust placement model as well.
- The power factor of all wind farms is considered to be 1.
- A DC power flow representation is adopted and line losses are neglected.

B. General model description

The robust placement problem is a kind of optimization problem to decide on the location of SWDs in the transmission lines and specify the adjustment settings of the located SWDs. Accordingly, the objective function of the optimization model is to minimize the total SWDs' investment cost (IC) as well as the generation cost (GC). The deterministic SWD placement model based on DC power flow approximation in the form of MINLP can be defined by the following equations (1)-(9).

$$\underset{\Xi}{Min} \quad \sum_k \left(C_k^{SWD} z_k\right) + \sum_t \sum_g N_t^h \left(C_g P_{g,t}\right) \tag{1}$$

$$P_{g,t}^{\min} u_{gt} \le P_{g,t} \le P_{g,t}^{\max} u_{gt} \quad \forall g,t \tag{2}$$

$$0 \le P_{wt} \le P_{f,wt} \quad \forall w,t \tag{3}$$

$$P_{gt} + P_{wt} - D_{nt} = \sum_{\forall k(n,m)} F_{k,t} - \sum_{\forall k(m,n)} F_{k,t} \quad \forall g,n,w,k,t \tag{4}$$

$$\begin{cases} F_{k,t} = \beta_{k,t} \cdot b_k \left(\theta_{n,t} - \theta_{m,t}\right) + b_k \left(\theta_{n,t} - \theta_{m,t}\right)\left(1 - z_k\right) \\ \theta_{(n=1),t} = 0 \quad \forall n,k,t \end{cases} \tag{5}$$

$$F_k^{\min} \le F_{k,t} \le F_k^{max} \quad \forall k,t \tag{6}$$

$$\theta_n^{\min} \le \theta_{n,t} \le \theta_n^{max} \quad \forall n,t \tag{7}$$

$$z_k \le \beta_k \le \beta_k^{\max} z_k \quad \forall k,t \tag{8}$$

$$\sum_k z_k \le \eta, \quad z_k \in \{0,1\} \tag{9}$$

where Ξ is $\{P_{g,t}, P_{wt}, F_{k,t}, \theta_{n,t}, \beta_k, z_k\}$. The objective function (OF) (1) minimizes the investment cost (IC) of SWDs in addition to generation cost (GC). The limits of the generating units and wind power generation are represented by (2) and (3), respectively. Constraint (4) refers to the nodal power balance for each bus. Constraint (15) represents the power flow of each transmission line as a function of the angle difference of connected buses and the compensation level provided by a SWD. The right-hand side of (5) consists of two parts. The first part is nonzero only when the line is selected for compensation, i.e., $z_k = 1$; and the second part, i.e., b_k ($\theta_{n,t}$ - $\theta_{m,t}$), applies to all transmission lines. Note that β_k is a variable in the constraint (5). Accordingly, this constraint is nonlinear, because it includes the multiplication of ($\theta_{n,t}$ and β_k) or ($\theta_{n,t}$ and z_k). Additionally, in constraint (5), the phase angle of the reference bus is fixed to zero. The grid limitations including line power flow limit and bus angle have been formulated in constraints (6) and (7), respectively. Possible compensation limits of the SWD is mentioned by constraint (8). Noted that, constraint (8) increases line impedance. Constraint (9) limits the number of SWDs that can be located in the transmission lines.

C. Robust SWD placement formulation

To include the security constraints in the proposed formulation of SWD placement problem to take care of wind uncertainty set (10), the constraints (10)–(17) are defined.

$$U\left(P_{f,wt}, \overline{P}_{wt}, \Delta\Theta_w\right) := \left\{ \begin{array}{l} \sum_w \sum_t \left| \dfrac{P_{wt}^u - P_{f,wt}}{\overline{P}_{wt}} \right| \le \Delta\Theta_w \\ P_{f,wt} + \overline{P}_{wt} \le P_{wt}^u \le P_{f,wt}^b + \overline{P}_{wt}; \forall w,t \end{array} \right\} \tag{10}$$

$$-\Delta r_{g,t} u_{gt} \le P_{g,t}^u - P_{gt} \le \Delta r_{g,t} u_{gt} \quad \forall g,t \tag{11}$$

$$0 \le P_{wt}^u \le P_{f,wt} \quad \forall w,t \tag{12}$$

$$P_{gt}^u + P_{wt}^u - D_{nt} = \sum_{\forall k(n,m)} F_{k,t}^u - \sum_{\forall k(m,n)} F_{k,t}^u \quad \forall g,n,w,k,t \tag{13}$$

$$\begin{cases} F_{k,t}^u = \beta_{k,t}^u b_k \left(\theta_{n,t}^u - \theta_{m,t}^u\right) + b_k \left(\theta_{n,t}^u - \theta_{m,t}^u\right)\left(1 - z_k\right) \\ \theta_{(n=1),t}^u = 0 \quad \forall n,k,t \end{cases} \tag{14}$$

$$F_k^{\min} \le F_{k,t}^u \le F_k^{max} \quad \forall k,t \tag{15}$$

$$\theta_n^{\min} \le \theta_{n,t}^u \le \theta_n^{max} \quad \forall n,t \tag{16}$$

$$z_k \le \beta_{k,t}^u \le \beta_k^{max} z_k \quad \forall k,t \tag{17}$$

The uncertainty set denoted by U includes wind power forecast $P_{f,wt}$ and its forecast error $\overline{P}_{wt}$, uncertainty budget level of WPG, $\Delta\Theta_w$. Since, the forecast values of WPG, $P_{f,wt}$ could be inaccurate, P_{wt}^u is used to represent possible WPG realization which taking value contained by the uncertainty interval, i.e., $P_{wt}^u \in \left[P_{f,wt} - \overline{P}_{wt}, P_{f,wt} + \overline{P}_{wt}\right]$. In (10), the constraint $\sum_w \sum_t \left| \frac{P_{wt}^u - P_{f,wt}}{\overline{P}_{wt}} \right| \le \Delta\Theta_w$ controls the total deviation of WPG from its forecasted value throughout the operation horizon wherein $\Delta\Theta_w$ takes a value between 0 and 1. When this parameter fixed to zero, the uncertainty set is converted to the deterministic case which neglects the uncertainty of WPG. As this parameter increases, the total deviation from the wind power forecast will be increased. Constraint (11) makes bundling between the deterministic and stochastic scenarios to impose remedial solution arrangements by adjusting the power output in both up and down sides, i.e., $\Delta r_{g,t}$. Constraints (12)–(17) represent the response of equations (3)–(8) to wind uncertainty, where the variables P_g, P_{wt}, $F_{k,t}$, $\theta_{n,t}$ and $\beta_{k,t}$ are replaced by P_g^u, P_{wt}^u, $F_{k,t}^u$, $\theta_{n,t}^u$ and β_k^u, respectively. Note that, (14), similar to (5), is a nonlinear constraint that makes (1)–(17) an MINLP. The terms $\beta_{k,t} b_k \left(\theta_{n,t} - \theta_{m,t}\right)$ and $b_k \left(\theta_{n,t} - \theta_{m,t}\right)\left(1 - z_k\right)$ in constraint (5) and (14) are nonlinear. So, to overcome the nonlinearity of these terms, we introduce two new variables, as shown in (18) and (19).

$$\Psi_{k,t} = \beta_{k,t} b_k \left(\theta_{n,t} - \theta_{m,t}\right) \tag{18}$$

$$F_{k,t} = b_k \left(\theta_{n,t}^u - \theta_{m,t}^u\right)\left(1 - z_k\right) \tag{19}$$

The new variable $\Psi_{k,t}$ represents the power flow in the transmission line as a result of installing SWD. By substituting this new variable for the two order polynomial, we are lifting the two order polynomial equation into a higher dimensional space and overcoming its nonlinearity. Upon attaining the solution in the higher dimensional space, it is projected back to

This article has been accepted for publication in a future issue of this journal, but has not been fully edited. Content may change prior to final publication. Citation information: DOI 10.1109/TSTE.2018.2877106, IEEE Transactions on Sustainable Energy

the original space to obtain the solution of the polynomial. Since this new variable contains a binary variable, a disjunctive model is considered to ensure that while the binary variable is zero the new variable is also zero. In addition, since the compensation level is positive, i.e., $\beta_{k,t}>0$, the sign of $\Psi_{k,t}$ and $\theta_{n,t}-\theta_{m,t}$ should be the same. Specifically, the following constraints need to be satisfied:

$$if \quad (\theta_{n,t}-\theta_{m,t})>0: \quad then \quad \Psi_{k,t}>0 \tag{20}$$

$$if \quad (\theta_{n,t}-\theta_{m,t})<0: \quad then \quad \Psi_{k,t}<0 \tag{21}$$

The "if conditions" in constraints (20) and (21) can be modeled by defining a new binary variable, i.e., $\upsilon_{k,t}$. While the value of $\upsilon_{k,t}$ is one, both $\Psi_{k,t}$ and $\theta_{n,t}-\theta_{m,t}$ are negative; and while the value of $\upsilon_{k,t}$ is zero, both $\Psi_{k,t}$ and $\theta_{n,t}-\theta_{m,t}$ are positive. Therefore, $\upsilon_{k,t}$ has been added to surrogate the signs of $\Psi_{k,t}$ and $\theta_{n,t}-\theta_{m,t}$. Furthermore, once the optimal value of the binary variable, $\upsilon_{k,t}$, are identified, the complexity of the optimization would be reduced. It should be noted that identifying the direction of the power flow on the transmission lines is very important to reduce solution time. Accordingly, constraints (5) and (14) can be reformulated as MILP using a big number technique, *M,* as follows:

$$-M(1-\upsilon_{k,t})\le\Psi_{k,t}\le M\upsilon_{k,t} \tag{22}$$

$$-M(1-\upsilon_{k,t})\le(\theta_{n,t}-\theta_{m,t})\le M\upsilon_{k,t} \tag{23}$$

$$\begin{cases}\Psi_{k,t}\ge-\beta_k^{\max}b_k(\theta_{n,t}-\theta_{m,t})-M(1-z_k)\\ \Psi_{k,t}\le\beta_k^{\max}b_k(\theta_{n,t}-\theta_{m,t})+M(1-z_k)\end{cases} \tag{24}$$

$$-F_k^{\max}(z_k)\le\Psi_{k,t}\le F_k^{\max}(z_k) \tag{25}$$

Eq. (18) is linearized by (22)—(25). But, (19) is linearized by a disjunctive model (26)—(28). In these equations, once $z_k=1$ indicates that SWD is installed on line *k,* $F_{k,t}$ is 0 and also once $z_k=0$ indicate that SWD is not installed on line *k,* $F_{k,t}$ limits between $-F_k^{\max}$ and $F_k^{\max}$. Finally, by substituting $\Psi_{k,t}$ and $F_{k,t}$ in nonlinear (28), this equation converts to a linear equation.

$$b_k(\theta_{n,t}-\theta_{m,t})-M(z_k)\le F_{k,t}\le b_k(\theta_{n,t}-\theta_{m,t})+M(z_k) \tag{26}$$

$$-F_k^{\max}(1-z_k)\le F_{k,t}\le F_k^{\max}(1-z_k) \tag{27}$$

$$P_{gt}+P_{wt}-D_{nt}=\sum_{\forall k(n,m)}(F_{k,t}+\Psi_{k,t})-\sum_{\forall k(m,n)}(F_{k,t}+\Psi_{k,t}) \tag{28}$$

IV. Proposed Solution Approach

The proposed solution approach (PSA) includes two main parts: a tri-stage decomposed optimization problem (named Part I) and a heuristic fast-tracking prescreening procedure (named Part II) to select the candidate lines to install SWDs.

A. *Part* I: Tri-Stage decomposition approach

Even a small number of the proposed robust SWD placement model (1)-(17) for small power systems cannot be solved using available commercial solution strategies like branch-and-cut or -bound solvers. Nevertheless, increasing the number of SWDs to be placed in the system will directly increase the size of the problem which may cause intractability. However, by means of decomposition approach, the robust SWD placement formulation (1)-(17) can be decomposed into a master problem and tractable subproblems (SPs) I and II, to be solved individually with the reduced computational burden. Accordingly, to solve the proposed SWD placement problem, a tri-stage decomposition approach is proposed as follows:

Master problem: The part of the problem, MP, minimizes the objective function (1) while considering (2) – (3), (7) – (9), (22) – (28) as constraints as well as all feasibility benders cuts obtained so far. No feasibility bender cuts exist in the first main iteration. In further main iterations, the MP does not create additional variables, but it includes new feasibility bender cuts from subproblems I and II, for deriving new P_{gt}/z_k for withstanding wind power uncertainty.

SP-I (*Identifying the worst-case realizations*): The minimum violation once that wind power varies within its uncertain interval is specified by a max-min optimization problem (29) subject to constraints (30) for calculating the largest minimum violation.

$$\max_{\Theta}\min_{\Xi}\sum_t\sum_n(\Phi_{1,nt}+\Phi_{2,nt}) \tag{29}$$

$$\begin{cases}-P_{g,t}^u\le\Delta r_{g,t}\hat{u}_{gt}-\hat{P}_{gt}, & \forall g,t\\ P_{g,t}^u\le\Delta r_{g,t}\hat{u}_{gt}+\hat{P}_{gt}, & \end{cases}\quad \begin{matrix}\underline{\ell}_{1,gt}\\ \overline{\ell}_{2,gt}\end{matrix} \tag{30a}$$

$$0\le P_{w,t}^u\le P_{f,wt}^u,\quad \forall w,t \qquad \overline{\ell}_{3,wt} \tag{30b}$$

$$P_{gt}^u+P_{wt}^u-\sum_{\forall k(n,m)}(F_{k,t}^u+\Psi_{k,t}^u)+\sum_{\forall k(m,n)}(F_{k,t}^u+\Psi_{k,t}^u)-\Phi_{1,nt}+\Phi_{2,nt}=D_{nt}, \quad \forall g,n,w,k,t \qquad \ell_{4,nt} \tag{30c}$$

$$\begin{cases}-F_{k,t}^u+b_k(\theta_{n,t}^u-\theta_{m,t}^u)\le M(\hat{z}_k),\\ F_{k,t}^u-b_k(\theta_{n,t}^u-\theta_{m,t}^u)\le M(\hat{z}_k),\end{cases}\forall n,m,k,t \quad \begin{matrix}\underline{\ell}_{5,kt}\\ \overline{\ell}_{6,kt}\end{matrix} \tag{30d}$$

$$\begin{cases}-F_{k,t}^u\le F_k^{\max}(1-\hat{z}_k),\\ F_{k,t}^u\le F_k^{\max}(1-\hat{z}_k),\end{cases}\forall k,t \quad \begin{matrix}\underline{\ell}_{7,kt}\\ \overline{\ell}_{8,kt}\end{matrix} \tag{30e}$$

$$\begin{cases}-\Psi_{k,t}\le M(1-\hat{\upsilon}_{k,t}),\\ \Psi_{k,t}\le M\hat{\upsilon}_{k,t},\end{cases}\forall n,k,t \quad \begin{matrix}\underline{\ell}_{9,kt}\\ \overline{\ell}_{10,kt}\end{matrix} \tag{30f}$$

$$\begin{cases}-\Psi_{k,t}-\beta_k^{\max}b_k(\theta_{n,t}-\theta_{m,t})\le M(1-\hat{z}_k),\\ \Psi_{k,t}-\beta_k^{\max}b_k(\theta_{n,t}-\theta_{m,t})\le M(1-\hat{z}_k),\end{cases}\quad \begin{matrix}\underline{\ell}_{11,kt}\\ \overline{\ell}_{12,kt}\end{matrix} \tag{30g}$$

$\forall n,m,k,t$

$$\begin{cases}-\Psi_{k,t}\le F_k^{\max}(\hat{z}_k),\\ \Psi_{k,t}\le F_k^{\max}(\hat{z}_k),\end{cases}\forall k,t \quad \begin{matrix}\underline{\ell}_{13,kt}\\ \overline{\ell}_{14,kt}\end{matrix} \tag{30h}$$

$$\begin{cases}-\beta_{k,t}^u\le-\hat{z}_k,\\ \beta_{k,t}^u\le\beta_k^{max}\hat{z}_k,\end{cases}\forall k,t \quad \begin{matrix}\underline{\ell}_{15,kt}\\ \overline{\ell}_{16,kt}\end{matrix} \tag{30i}$$

$$\begin{cases}-\theta_{n,t}^u\le-\theta^{\min},\\ \theta_{n,t}^u\le\theta^{max},\\ \theta_{n=1,t}^u=0,\end{cases}\quad \forall n,t \quad \begin{matrix}\underline{\ell}_{17,nt}\\ \overline{\ell}_{18,nt}\\ \ell_{19,t}\end{matrix} \tag{30j}$$

where Θ and Ξ are $\{P_{f,wt}^u\}$ and $\{P_g,P_w,F,\theta,\beta,\Psi,\Phi\}$, respectively. To solve the above-mentioned *max–min* optimization problem, based on the duality theory, the dual form of the *min* part is extracted, and then we have a single maximization problem as follows:

$$\begin{aligned}\max_{\{P_{f,wt}^u\}}\ &\sum_g\left((\Delta r_{g,t}\hat{u}_{gt}-\hat{P}_{gt})\underline{\ell}_{1,gt}+(\Delta r_{g,t}\hat{u}_{gt}+\hat{P}_{gt})\overline{\ell}_{2,gt}\right)\\ &+\sum_w(P_{f,wt}^u\overline{\ell}_{3,wt})+\sum_n(D_{n,t}\overline{\ell}_{4,nt})+\sum_k(\overline{\ell}_{6,kt}+\underline{\ell}_{5,kt})M(\hat{z}_k)\\ &+\sum_k(\overline{\ell}_{7,kt}+\underline{\ell}_{8,kt})F_k^{max}(1-\hat{z}_k)\\ &+\sum_k(M(1-\hat{\upsilon}_{k,t})\underline{\ell}_{9,kt}+M\hat{\upsilon}_{k,t}\overline{\ell}_{10,kt})\\ &+\sum_k M(1-\hat{z}_k)(\underline{\ell}_{11,kt}+\overline{\ell}_{12,kt})+\sum_k F_k^{\max}(\hat{z}_k)(\underline{\ell}_{13,kt}+\overline{\ell}_{14,kt})\\ &+\sum_k F_k^{\max}(z_k)(-\hat{z}_k\underline{\ell}_{15,kt}+\beta_k^{max}\hat{z}_k\overline{\ell}_{16,kt})\\ &+\sum\theta^{max}(\overline{\ell}_{17,nt}-\underline{\ell}_{18,nt})\end{aligned} \tag{31}$$

s.t:

$$-\underline{\ell}_{1,gt}+\overline{\ell}_{2,gt}+\ell_{4,nt}\le0\quad\forall g,n,t \tag{32a}$$

$$\ell_{3,wt}+\ell_{4,nt}\le0\quad\forall n,w,t \tag{32b}$$

This article has been accepted for publication in a future issue of this journal, but has not been fully edited. Content may change prior to final publication. Citation information: DOI 10.1109/TSTE.2018.2877106, IEEE Transactions on Sustainable Energy

$$\left(\ell_{4,nt}-\ell_{4,mt}\right)+\left(\overline{\ell}_{6,kt}-\underline{\ell}_{5,kt}\right)+\left(\overline{\ell}_{8,kt}-\underline{\ell}_{7,kt}\right)\le 0,\forall g,n,m,k,t \quad (32c)$$

$$\left[\begin{array}{l}\left(\ell_{4,mt}-\ell_{4,nt}\right)+\left(\overline{\ell}_{10,kt}-\underline{\ell}_{9,kt}\right)+\\ \left(\overline{\ell}_{12,kt}-\underline{\ell}_{11,kt}\right)+\left(\underline{\ell}_{14,kt}-\underline{\ell}_{13,kt}\right)\end{array}\right]\le 0,\forall n,m,k,t \quad (32d)$$

$$-1\le \ell_{4,nt}\le 1,\forall n,t \quad (32e)$$

$$\left(\overline{\ell}_{16,kt}-\underline{\ell}_{15,kt}\right)\le 0,\forall k,t \quad (32f)$$

$$\begin{aligned}&\sum_{k(n,m)} b_k\underline{\ell}_{5,kt}-\sum_{k(m,n)} b_k\underline{\ell}_{5,kt}-\sum_{k(n,m)} b_k\overline{\ell}_{6,kt}\\ &+\sum_{k(m,n)} b_k\overline{\ell}_{6,kt}-\sum_{k(n,m)}\beta_k^{\max}b_k\underline{\ell}_{11,kt}+\sum_{k(m,n)}\beta_k^{\max}b_k\underline{\ell}_{11,kt},\forall n\ne 1,k,t\\ &-\sum_{k(n,m)}\beta_k^{\max}b_k\overline{\ell}_{12,kt}+\sum_{k(m,n)}\beta_k^{\max}b_k\overline{\ell}_{12,kt}+\overline{\ell}_{18,nt}-\overline{\ell}_{17,nt}\le 0\end{aligned} \quad (32g)$$

$$\begin{aligned}&\sum_{k(n,m)} b_k\underline{\ell}_{5,kt}-\sum_{k(m,n)} b_k\underline{\ell}_{5,kt}-\sum_{k(n,m)} b_k\overline{\ell}_{6,kt}\\ &+\sum_{k(m,n)} b_k\overline{\ell}_{6,kt}-\sum_{k(n,m)}\beta_k^{\max}b_k\underline{\ell}_{11,kt}+\sum_{k(m,n)}\beta_k^{\max}b_k\underline{\ell}_{11,kt}\\ &-\sum_{k(n,m)}\beta_k^{\max}b_k\overline{\ell}_{12,kt}+\sum_{k(m,n)}\beta_k^{\max}b_k\overline{\ell}_{12,kt}+\ell_{19,t}\le 0,\quad \forall n=1,k,t\end{aligned} \quad (32h)$$

$$\begin{cases}\underline{\ell}_{1,gt},\overline{\ell}_{2,gt},\overline{\ell}_{3,\mathrm{w}t},\underline{\ell}_{5,\mathrm{k}t},\overline{\ell}_{6,\mathrm{k}t},\underline{\ell}_{7,\mathrm{k}t},\overline{\ell}_{8,kt},\\ \underline{\ell}_{9,kt},\overline{\ell}_{10,\mathrm{k}t},\underline{\ell}_{11,kt},\overline{\ell}_{12,kt},\underline{\ell}_{13,kt},\overline{\ell}_{14,kt},\underline{\ell}_{15,kt},\overline{\ell}_{16,kt}\le 0\\ ,\underline{\ell}_{17,nt},\overline{\ell}_{18,nt}\\ \ell_{4,\mathrm{n}t},\ell_{19,t}\quad \text{unlimited},\forall g,n,w,k,t\end{cases} \quad (32i)$$

The maximization of the objective function (31) subject to constraints (32) is a bilinear optimization problem due to the product of decision variables in (31) (i.e., $P^{u}_{f,wt}\cdot\overline{\ell}_{3,wt}$). Different techniques can be deployed to resolve the bilinear optimization problem (31), such as interior-point methods [16] and an exact MILP reformulation [21]. In this paper, the $P^{u}_{f,wt}\cdot\overline{\ell}_{3,wt}$ is linearized by the proposed method in [21].

SP-II (*worst-case realization*): If the objective function (33) subject to constraints (34) violated the prespecified threshold, a new benders feasibility cut (35) will be created and provided for the MP for seeking robust scheduling and dispatching of generating units that would will consider the security for the entire uncertain intervals.

$$\min \Re^{worst}=\sum_t\sum_n(\vartheta_{1,nt}+\vartheta_{2,nt}) \quad (33)$$

$$\begin{aligned}&P_{gt}+P^{worst}_{wt}-\sum_{\forall k(n,m)}\left(F_{k,t}+\Psi_{k,t}\right)\\ &+\sum_{\forall k(m,n)}\left(F_{k,t}+\Psi_{k,t}\right)=D_{nt}+\vartheta_{1,nt}-\vartheta_{2,nt},\forall g,n,w,k,t\end{aligned} \quad (34a)$$

$$\text{(10)-(12), (17) and (19)-(25) for } P^{worst}_{w,t} \quad (34b)$$

$$z_k=\hat{z}_k\quad :\kappa^2_k\quad \forall k\ ,\ P_{gt}=\hat{P}_{gt}\quad :\kappa^1_{gt}\quad \forall g,t \quad (34c)$$

$$\hat{\Re}^{worst}+\sum_t\sum_g\kappa^1_{gt}\left(P_{gt}-\hat{P}_{gt}\right)+\sum_k\kappa^2_k\left(z_k-\hat{z}_k\right)\le 0 \quad (35)$$

where $\left\{\kappa^1_{gt},\kappa^2_k\right\}$ are dual variables corresponding to $\left\{P_{g,t},z_k\right\}$ variables shown in constraints (34c).

Finally, the algorithm of the tri-stage decomposition approach for the proposed problem works as follows:

Step I (MP): The MP minimizes the IC and GC (1) subject to constraints (2) – (3), (7) – (9), (22) – (28) and all feasibility benders cuts obtained so far. Also, once the solution process for this step is finished, the variables, $\left\{P_{gt},u_{gt}\right\}$ and $\left\{\upsilon_{k,t},z_k\right\}$ can be known for all of the units and transmission lines, respectively.

Step II (SP-I): In this step, the equations (31) and (32) is solved to identify the worst WPG uncertainty realization, $P^{worst}_{w,t}$, that would lead to the largest minimum violation when wind power varies within its interval.

Step III (SP-II): In this step, if the minimum violation (33) for the worst WEG realization, $P^{worst}_{w,t}$, is larger than the prespecified threshold, the benders feasibility cut (35) will be created and sent to Step I for seeking robust investment and generation solutions against security violations.

Convergence: The above iterative process will be stopped once the solution results of MP satisfy all the remaining constraints in the subproblems I and II. That is, no more feasibility cut is generated in Step III.

The flowchart of the proposed solution methodology is shown in Fig. 1.

B. The second part (*determining a priority list for installing SWD*)

To avoid excessive solution iterations for the large-scale practices, the placement of SWD on transmission lines is determined using some heuristics methods, such as our proposed transmission line ranking approach in Fig.1, to select a reduced number of line candidates for installing SWD, and to decrease the number of binary variables in the optimization formulation. The main idea of transmission line ranking approach is to install SWD on high ranking transmission lines, so that it can decrease generation cost by increasing the available transfer capability. In our proposed problem, parameter η in constraint (9), i.e., $\sum_k z_k\le\eta$, determines the number of installed SWDs. Based on this parameter, the rank of a transmission line for install SWD is determined in the priority list. So, at first, the value of parameter η fixed to 0, then, part I is solved to obtain *OF* which is called OF_b.

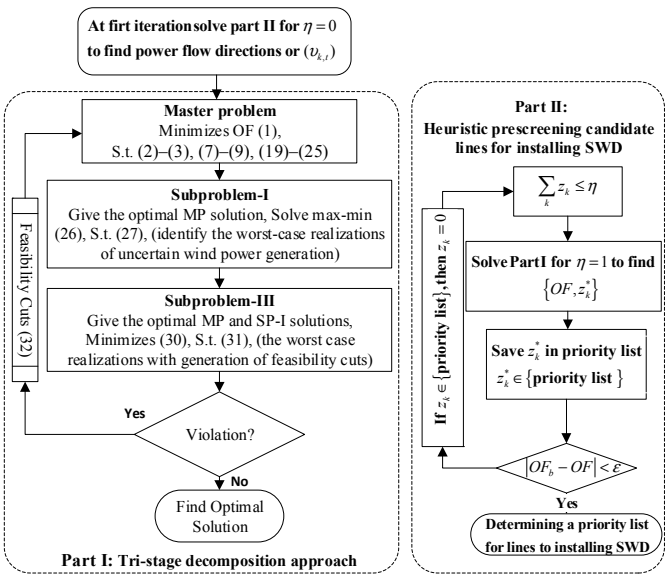

Fig.1. Proposed solution approach with Part II.

Then, the value of η is fixed to 1 and part I is solved at the first iteration. When a solution of part I finishes, a value for *OF* and a transmission line that equipped by a SWD are obtained. If the value of *OF* is less than OF_b (or $OF< OF_b$), then a transmission line that equipped by a SWD, i.e, z_k^*, has the first rank in the priority list which is saved in the priority list. Accordingly, to determine transmission line that has the second rank in priority list, previous transmission line that has the first rank removes from searched space, hence, the variable z_k^* for this transmission line is fixed to 0, and part I is solved for the second iteration. To determine the next transmission line that has the second rank in priority list also this transmission line is

This article has been accepted for publication in a future issue of this journal, but has not been fully edited. Content may change prior to final publication. Citation information: DOI 10.1109/TSTE.2018.2877106, IEEE Transactions on Sustainable Energy

saved in priority list. So, to determine other ranks in priority list the mentioned procedure is repeated to determine all rank of transmission line. Not that, before part I solves the variable z_k^*, for all the transmission lines in the priority list, should be fixed to 0. Finally, if $|OF - OF_b| \leq \varepsilon$ satisfies, then the process of solution problem stops.

In summary, the Part II for the proposed problem works as follows.

Step 1: The Part I is solved for $\eta=0$ *to* determine OF_b to the comparison.

Step 2: The value of η is fixed to 1 and a small tolerance ε is pre-selected to terminate the procedure.

Step 3: The Part I is solved for $\eta = 1$ to find OF (1) and z_k^*, then, the z_k^* is stored in the priority list to install SWD.

Step 4: If $|OF_b - OF| < \varepsilon$ is not satisfied, then, all stored z_k^* in the priority list are set to zero, to remove these transmission lines from the solution search space, and the procedure repeated with remaining lines until $|OF_b - OF| < \varepsilon$ is fully satisfied.

Step 5: the priority list for the line candidates to install SWDs is determined.

C. *Proposed solution algorithm*

Finally, according to the above-mentioned algorithms, the PSA can be summarised as the following algorithm:

Step I: The Part I without allocation SWD (i.e., η is fixed to 0) is solved then, the power flow directions through all lines, $v_{k,t}$, are determined.

Step II: The second part of Fig. 1 is taking place. Subsequently, the power flow directions, $\hat{v}_{k,t}$, are set to their values determined in Part I. Now, the priority list for the location of SWD is determined.

Step III: Finally, the first part (Part I) should be solved to find optimal locations of the SWD based on the priority list, then the process of solution problem will be stopped.

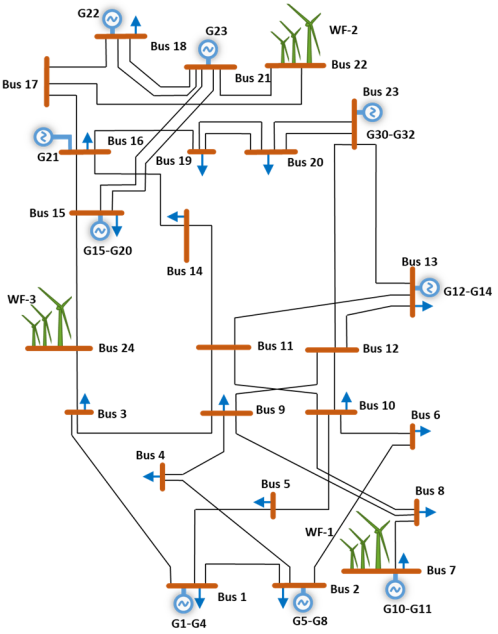

Fig. 2. IEEE One Area RTS-96.

V. Numerical Results

A. *Test system specifications*

The performance of the proposed model is evaluated using a slightly modified RTS-96 test system [22]. The test system includes 17 loads, 32 thermal units, and 38 transmission branches, with 6 hydro-units which are removed in this test system and replaced by a wind farm (as shown in Fig.2). Additional data about this system can be found in [22]. The SWD installing cost is considered equal to \$2200/km, with the annualized investment cost equal to 10% of the total cost. Further information about the capital cost of the SWD installation can be found in [7]. The SWDs are capable of operating in inductive mode only. Inductive adjustment of line's reactance has a great effect on the power flow results through rerouting power flow to underutilized transmission lines. The largest adjustment bound here, is ≤+10% to +40% of the line's reactance, as done in [7]. The demand and wind power levels for each block with its number of hours throughout the target year are provided in Table I, which have similar results as [23]. For each demand and wind block, the demand and wind power levels are multiplied by the peak demand and the installed wind power capacity, respectively, to obtain the actual demand and the maximum WPG for each block with its number of hours. In order to obtain a more realistic demand profile, it is assumed that the bus peak loads are 30% higher than their normal values, although the generation levels are about twice the values provided in [22]. Wind farms are available in 350-MW, 450-MW and 350-MW at buses 7, 22 and 24, respectively. The wind power output is obtained from the Wind Integration Datasets of NERL [24]. Since there are three wind farms and the model includes five time periods in the target year, the degree of the robustness can take different integer values between 0 and 3 × 5 = 15 (i.e., $0 \leq \Delta\Theta_w \leq 15$). The implement the proposed framework, the CPLEX 12.6 solver under GAMS optimization package [25] has been used by means of a PC with Intel Core-i7 processor at 4.2 GHz and 32 GB of RAM.

B. *Simulation results and discussion*

***Optimal Solution versus degree of robustness*:** The results obtained from the proposed adaptive robust SWD placement approach for the RTS-96 test system are illustrated in Fig. 3, considering different values for $\Delta\Theta_w$. The degree of robustness $\Delta\Theta_w$ can vary between 0 and 15. As Fig. 3 and Tables II to IV illustrate, GC and IC increase for a specific deviation from forecast values (e.g., $\bar{P}_{wt} = 0.25 \cdot P_{f,wt}$), as $\Delta\Theta_w$ is increased. The reasons for this fact are twofold: firstly, by increasing $\Delta\Theta_w$, a higher number of uncertain parameters can adopt their worst-case realizations resulting in a more robust and more expensive generation and investment state. However, once $\Delta\Theta_w = 0$, the uncertain wind parameters cannot deviate from their forecasted values (yielding the deterministic case). Consequently, the lowest GC and IC are imposed by $\Delta\Theta_w = 0$, as it ignores wind uncertainty. Besides, the GC increases with the rise of $\Delta\Theta_w$, which indicates that more units need to be committed to covering more wind farms uncertainties, and the robust SWD placement solution becomes more expensive. For instance, as can be seen in Table II, once $\Delta\Theta_w$ is increased from 0 to 15, more units are committed to mitigate a larger uncertainty or $\Delta\Theta_w = 15$. Alternatively, the IC increases with the rise of $\Delta\Theta_w$. For instance, with more $\Delta\Theta_w$, the power flow through the lines connected to bus 24 would be increased because of the installed wind farm at this bus. Accordingly, there may be some power flow violations in the lines connected to bus 24, e.g., power flow over lines 7 (between buses 3 and 24) and 27 (between buses 15–24). Therefore, to alleviate the violations of lines 7 and 27, inevitably, the expensive units 15 to 20 are committed. It is noted that these lines at most times are congested leading to the lower dispatch of wind farm in bus 24 and a higher generation cost. In order to mitigate the congestion over these lines, there are two remedial options: commitment of expensive units 15-20 and/or installing SWD. Both of them would lead to a decreasing the power flow of line 27. However, since using only the expensive units 15-20 is a costly choice here, installing SWD at line 7 along with the commitment of expensive units 15-20 would be the optimal choice. In this regard, the results of Tables III and IV, show the same conclusion. In these tables, for the case of $\Delta\Theta_w = 0$, $\eta = 1$, the line 28 (16-17) has been selected for compensation, but, for the case $\Delta\Theta_w = 15$ and $\eta = 1$, line 28 is replaced by line 7. The

This article has been accepted for publication in a future issue of this journal, but has not been fully edited. Content may change prior to final publication. Citation information: DOI 10.1109/TSTE.2018.2877106, IEEE Transactions on Sustainable Energy

investment cost of line 7 is more expensive than the line 28 that would lead to a higher investment cost.

TABLE I
DEMAND AND WIND LEVELS PER BLOCK

No. Block	Number of hours	Demand level (p.u.)	Wind intensity (p.u.)
1	1000	0.914	0.523
2	3000	0.773	0.545
3	3000	0.637	0.494
4	1000	0.480	0.583
5	760	0.337	0.613

TABLE II
THE SOLUTIONS OF UNIT COMMITMENT (UC) FOR $\Delta\Theta_w = 0$ AND 15.

	$\Delta\Theta_w = 0$					$\Delta\Theta_w = 15$				
	Demand block					Demand block				
Units	**1**	**2**	**3**	**4**	**5**	**1**	**2**	**3**	**4**	**5**
1	**1**	0	0	0	0	1	0	0	0	0
2	1	0	0	0	0	1	0	0	0	0
3	1	1	1	0	0	1	1	1	1	1
4	1	1	1	0	0	1	1	1	1	1
5	1	0	0	0	0	1	0	0	1	0
6	1	0	0	0	0	1	0	0	1	0
7	1	1	1	1	0	1	1	1	1	1
8	1	1	1	1	0	1	1	1	1	1
9	0	**1**	0	0	0	**1**	0	0	0	0
10	1	1	0	0	0	**1**	0	0	0	0
11	1	1	0	0	0	**1**	0	0	1	0
12	1	**1**	0	0	0	1	1	0	1	0
13	1	0	0	0	0	1	1	0	0	0
14	1	1	0	0	0	1	1	0	0	0
15	0	0	0	0	0	1	0	1	1	1
16	0	0	0	0	0	1	0	1	1	1
17	0	0	0	0	0	1	0	1	1	1
18	0	0	0	0	0	1	0	1	1	1
19	0	0	0	0	0	1	0	1	1	1
20	1	1	0	0	0	1	**0**	1	1	**0**
21	1	1	1	1	**1**	1	1	1	0	**0**
22	1	1	1	1	1	1	1	1	0	**0**
23	1	1	1	1	1	1	1	1	1	1
30	1	1	1	1	0	1	1	1	1	**0**
31	1	1	1	1	0	1	1	1	1	1
32	1	1	1	0	0	1	1	1	1	0
Total	**20**	**16**	**10**	**7**	**3**	**26**	**13**	**16**	**18**	**11**

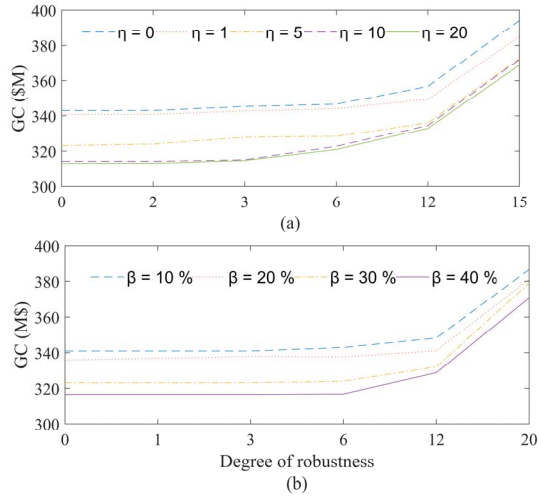

Fig. 3. Generation cost changes versus the degree of robustness for different (a) μ and (b) β.

TABLE III
OPTIMAL SOLUTION OF THE PROPOSED MODEL FOR A DIFFERENT NUMBER OF INSTALLED SWDS; $\beta^{max} = 1.15$ AND $\Delta\Theta_w = 0$.

η	Line No.	GC (M$/yr)	IN (M$/yr)	Time (Sec.)
1	28	338.03	2.24	1
2	7,23	324.84	12.03	3
4	4,7,23,28	318.08	14.47	9
8	7,8,17,23,28	314.25	18.27	10
10	7,8,17,23,28	314.25	18.27	20

4 (2-4), 6 (3-9), 7 (3-24),8 (4-9),10 (6-10), 13 (8-10), 17 (10-12), 20 (12-13), 23 (14-16), 28 (16-17), 38 (21-22)

TABLE IV
OPTIMAL SOLUTION OF THE PROPOSED MODEL FOR A DIFFERENT NUMBER OF INSTALLED SWDS; $\beta^{max} = 1.15$ AND $\Delta\Theta_w = 15$.

η	SWD location	Generation cost (M$/yr)	Investment cost (M$/yr)
1	7	375.258	6.198
2	7,17	374.185	9.894
4	7,8,17,38	371.307	13.184
8	6,7,8,13,17,20,27,38	370.507	36.523
10	6,7,8,10,13,17,20,23,27,38	363.471	44.419

TABLE V
OPTIMAL SOLUTION OF THE PROPOSED MODEL FOR A DIFFERENT NUMBER OF INSTALLED SWDS; $\beta^{max} = 1.30$ AND $\Delta\Theta_w = 15$.

η	SWD location	Generation cost (M$/yr)	Investment cost (M$/yr)	CPU time (Sec.)
1	7	370.86	6.19	30
2	7,20	366.02	19.39	87
4	7,8,17,23	358.99	27.67	160
8	6,7,8,17,23,27,30,38	354.82	24.22	210
10	6,7,8,17,23,27,30,38	352.00	24.22	320

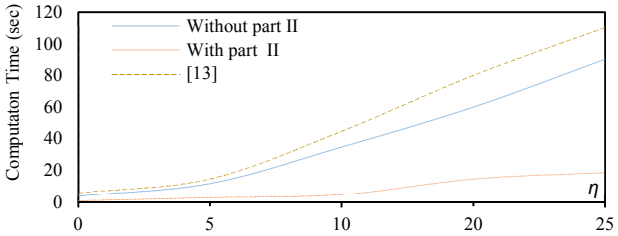

Fig. 4. Computation time comparison of PSA without and with part II, and in [13].

***Impact of SWD on the optimal solution*:** As can be seen, in Fig. 3 (a), without any SWD in the test system, i.e., $\Delta\Theta_w = 0$ and $\eta = 0$, the GC is M$343.74/yr. Results show that while $\eta = 0$ and $\Delta\Theta_w = 0$, one transmission line is congested, i.e., line 28 (16-17). The optimal SWD placement strategy while $\eta = 1$ and $\Delta\Theta_w = 0$ resulted in GC of M$338.03/yr implying 1.45% decrease in the cost in comparison with the case $\eta = 0$.

Furthermore, in this condition, IC is M$ 2.24 /yr. On the other hand, results show that while $\eta = 0$ and $\Delta\Theta_w = 0$, five transmission lines, in particular line 7 (3-24), are congested. For this reason, the SWD is installed in line 7 to enhance the flow capacity of line 27 and to increase the generation share of the cheaper wind farm at bus 24.

Compared to the results of $\eta = 1$ and $\Delta\Theta_w = 0$, although the GC decreases by M$23.35/yr, the IC increases by $6.19/y; however, the changes of IC is not as much as savings in GC. The results, in Fig. 3 (a), show the inclusion of SWDs reduces the GC, although the IC increases, their impact diminishes as the number of installed SWDs increases. For example, as shown in Fig.2 (a), for $\Delta\Theta_w = 15$, when η is 10 and 20, the GCs are M$314.257/yr and M$313.057/yr, respectively. Noted that $\eta = 20$ has a minor influence on the GC reduction. Finally, the following observations can be inferred from Fig.2 (a) and Tables II to IV:

- To compare the GC and IC of SWD, Fig.2 (a) indicates the results of the proposed model for η from 1 to 15. The highest decrease in the GC occurs while η increased from 1 to 10 which is M$ 22.175 /yr. Meanwhile, the highest increase in IC also occurs at the same time. Fig. 3 (a) proves that the highest decrease in the GC attained by installing SWDs while $\eta = 20$ which is equal to M$ 25.429 /yr. This value is slightly lower than M$ 22.175 /yr which is the savings when η=10.
- As the number of SWDs increases, more inexpensive units are used which results in the lower total cost. For instance, as can be seen in Table II, for $\Delta\Theta_w = 15$, the expensive units 9-11 and inexpensive units 20-22 are on-line and off-line for $\eta = 0$, respectively, but, for $\eta = 10$, these units are off-line and on-line, respectively. The changes in the

This article has been accepted for publication in a future issue of this journal, but has not been fully edited. Content may change prior to final publication. Citation information: DOI 10.1109/TSTE.2018.2877106, IEEE Transactions on Sustainable Energy

commitment of units for η = 0 compared to η = 10 in $\Delta\Theta_w = (0,15)$, are bolded and highlighted in Table II.

***Impact of compensation level (β) on the optimal solution*:** Fig. 3 (b) shows the GC as a function of a line's compensation level β and for η = 10. The proposed model is solved for η = 10 and β value increases by a step size of 10% from 10% to 40%. The optimal placements of SWD for $\Delta\Theta_w$ = 15 and β=1.15 to 1.3 are shown in Tables IV and V. Interesting insights can be inferred from Fig. 3 (b) and Tables IV and V.

- The GC is decreased by increase β value, (Fig.2 (b)).
- The impact of compensation weakens as the degree of the robustness increases, i.e., $\Delta\Theta_w$ = 0 to 15, (Fig.2 (b)).
- The locations of the SWD in most cases with variation compensation level (β) changed with the same number of
- SWD and degree of robustness (i.e., with η = 10 and $\Delta\Theta_w$ = 15), (shown in Tables IV and V).
- By comparing the results of Tables IV and V, it is observed that by increasing β from 1.15 to 1.3, the number of SWD reduces for some cases; while η is the same. Besides, the results show that once the β value increases, the IC and GC will decrease.

Also, the results suggest that the optimal set point of β, may affect the optimal SWD placement. It is, therefore, necessary to consider the optimal set point of β in the long-term SWD placement to ensure that the maximum return on the investment will be achieved. Also, the SWDs by increasing the line impedances offer some kinds of flexibility for the transmission system and can be heavily influenced by applying compensation level (β).

The results of this comprehensive search indicate the lowest GC is obtained when β is equal to 1.4 or 40%, (as shown in Fig.2 (b)). In conclusion, it is, therefore, necessary to consider β and $\Delta\Theta_w$ values when choosing the lines for SWD placement in the planning phase to obtain better economic savings in the future generation costs.

***Computational Performance of the proposed solution approach*:** To show the computational performance of the PSA in handling the larger number of the SWDs, the proposed robust SWD placement with solution strategy in [13] and the PSA with and without part II are compared. The number of SWD is changed from η = 1 to 25 with the step of 5. Where η = 25 means that more than half of the transmission lines in the system are candidates for the SWD placement. Fig. 4., summarizes the computational performance of the PSA with part II as compared to the performance of the other solution approaches, i.e., PSA while ignoring part II and the presented method in [13]. Noted that, the difference between the CG and IC of three models are negligible and also the locations of SWDs in three methods are the same. But, the PSA obtains the lowest GC compared to other solution strategies. In Fig. 4, for a small number of SWDs, three solution strategies find the optimal solution in a reasonable time, i.e., for η < 10. However, as illustrated in the figure, the PSA without part II and solution strategy in [13] fail to deal with the proposed robust placement model considering a high number of SWDs, i.e., for η > 10. For instance, for η = 10, the solution time to get the optimal results for the PSA with part II is 5 Sec with respect to 35 Sec and 45 Sec of the PSA without part II and solution in [13], respectively. However, as we increase the number of SWDs, the execution time of the PSA while ignoring part II and the presented method in [13] increases significantly, while that of our PSA with part II remains reasonable. In the case of η = 25, the optimal solution of the PSA is obtained in 19 sec, while that of two other solution strategies are achieved in more than 100 sec. This considerable increase in execution time is due to a large number of binary variables that should be handled by the two other solution strategies. However, in the PSA with part II, these binary variables are decreased by Part II. As can be seen in the obtained results, the PSA in the presence of part II would help tri-stage decomposition approach to have an acceptable execution time. Finally, as can be seen in Fig.3, it is clear that robust SWD placement using PSA with part II is much more efficient than using two other solution approaches.

***Comparing the proposed robust approach with other robust approaches on a modified IEEE 118-bus system*:** In this case, the performance of our proposed three-stage robust approach and the robust approach in [16] has been compared to handle the wind uncertainty on IEEE 118-bus test system. The IEEE 118-bus test system as a more realistic and larger test system is used here, to represent the performance of our proposed RA and RA [16] against the scale of the test system. Here, the modified IEEE 118-bus system is used to show the effectiveness of the proposed RA, which includes 54 thermal units, 186 lines, and 91 loads and three wind farms, [motor.ece.iit.edu/data/SCUC_118]. Accordingly, three 600-MW wind farms are connected to buses 17, 49 and 96. Since there are three wind farms and the model includes five time periods in the target year (similar to the previous test system), the degree of the robustness can adopt different integer values between 0 and 3 × 5 = 15 (i.e., $0 \le \Delta\Theta_w \le 15$). In this study, the proposed adaptive RA and the other RA in [16], to handle the wind uncertainty in the proposed adaptive robust SWD placement problem, are compared in three aspects: 1) the IC and OC, 2) location of SWD and 3) computation time. The performance of the two approaches under different η value and with constant wind uncertainty budget level ($\Delta\Theta_w$ = 15) are also investigated. Table VI reports the IC and OC of the proposed RA and the RA in [16] with respect to different η value. As can be seen in Table VI, once the number of installed SWDs increases, the IC and OC for both approaches are increasing and decreasing, respectively, because more SWD need to be installed and also more thermal units need to be committed to cover a wider range of wind uncertainties. Once η is 1, the IC of the two methods is the same, but the OC for the proposed RA is lower than the RA in [16].

TABLE VI
OPTIMAL SOLUTION OF THE PROPOSED RA AND RA [16] FOR A DIFFERENT η; β^{max} = 1.15 AND $\Delta\Theta_w$ = 15.

	η	SWD bus-bus	GC (M$/yr)	IC (M$/yr)	CPU time (min)
Proposed RA	**1**	94-100	523.678	4.58	5
	2	94-100, 17-18	492.231	8.43	8
	4	94-100,49-54, 17-113,96-93	471.678	19.67	12
RA [16]	**1**	94-100	589.761	4.58	26
	2	94-100, 49-69	516.342	10.43	43
	4	94-100,49-69, 49-66,17-113	491.443	27.65	65

Differences in the OCs are mainly caused by the ways on how these two RAs handle uncertainties. In the proposed RA, the system is considered to be operated under the base case with unit dispatch and commitment decisions corresponding to the forecasted values and in the day-ahead scheduling, and thermal units output are securely and adaptively adjusted based on corrective capabilities of thermal units once possible realizations of wind uncertainties occur in real time. For the RA in [16], the system is intended to be operated only with UC decisions corresponding to the worst case uncertainty in the operation stage, and thermal units output is adaptively determined based on the robust UC decisions once possible realizations of wind uncertainties occur.

The basic idea is that if a UC solution could manage the worst case uncertainty, it could be able to find a secure dispatch solution for managing any uncertainty. In summary, the savings in the OCs is caused by the robust thermal unit dispatch and commitment solutions corresponding to the base case and the corrective capabilities of thermal units in the proposed model, as compared to the RA solutions corresponding to the worst

case uncertainty in [16]. Also as shown in Table VI, the location of SWD, for $\eta>1$, is different for both RA approaches. But, the proposed RA selects more economic and appropriate locations than the RA in [16]. On the other hand, as we increase the η value, the execution time of the PSA and the RA in [16] increases significantly, while that of our proposed RA remains reasonable. Finally, the SWD placement problem with our proposed RA could provide more economic and reliable SWD placement and thermal units operation.

VI. Conclusion

The SWD technology as a kind of grid side flexibility can be harnessed to accommodate higher capacities of wind power generation. This paper proposed an adaptive robust max–min SWD placement model for power systems with WPG uncertainty. The robust SWD placement solution was immunized against different realizations of uncertain WPG within the forecasted uncertainty interval (set). While the proposed robust SWD placement is in the form of MINLP, a modified disjunctive method has been proposed to convert it to tractable MILP form. The objective function of the model minimized the generation and investment costs while considering wind uncertainty. Since there was no available off-the-shelf optimization package to solve the suggested max–min model, an efficient solution approach has been proposed in this work, which is based on a tri-level decomposition algorithm along with the innovative pre-screening procedure to select candidate lines for installing SWDs. Finally, the IEEE 24-bus was used to test the performance of the proposed procedure and enhance our understanding of the robust SWD placement problem. The results showed:

- It is pointed out that the GC and IC increased as the degree of robustness or the respective variation range of the uncertain wind power increased.
- Increasing the reactance of a certain transmission line (by SWDs) could reduce the GC and IC for different degree of robustness.
- The degree of robustness and compensation levels had an effect on SWD placement. Consequently, it is essential to consider the degree of robustness in the placement phase for SWDs.

References

[1] M. E. Khodayar, M. Shahidehpour, and L. Wu, "Enhancing the dispatchability of variable wind generation by coordination with pumped-storage hydro units in stochastic power systems," *IEEE Transactions on Power Systems,* vol. 28, no. 3, pp. 2808-2818, 2013.

[2] J. Aghaei, A. Nikoobakht, M. Mardaneh, M. Shafie-khah, and J. P. Catalão, "Transmission switching, demand response and energy storage systems in an innovative integrated scheme for managing the uncertainty of wind power generation," *International Journal of Electrical Power & Energy Systems,* vol. 98, pp. 72-84, 2018.

[3] D. Das, F. Kreikebaum, D. Divan, and F. Lambert, "Reducing transmission investment to meet renewable portfolio standards using smart wires," in *Transmission and Distribution Conference and Exposition, 2010 IEEE PES*, 2010, pp. 1-7: IEEE.

[4] M. Sahraei-Ardakani and K. W. Hedman, "A fast LP approach for enhanced utilization of variable impedance based FACTS devices," *IEEE Transactions on Power Systems,* vol. 31, no. 3, pp. 2204-2213, 2016.

[5] M. Sahraei-Ardakani and K. W. Hedman, "Computationally Efficient Adjustment of FACTS Set Points in DC Optimal Power Flow with Shift Factor Structure," *IEEE Transactions on Power Systems,* vol. 32, no. 3, pp. 1733-1740, 2017.

[6] F. Kreikebaum, D. Das, Y. Yang, F. Lambert, and D. Divan, "Smart wires—a distributed, low-cost solution for controlling power flows and monitoring transmission lines," in *Innovative Smart Grid Technologies Conference Europe (ISGT Europe), 2010 IEEE PES*, 2010, pp. 1-8: IEEE.

[7] N. Rani, P. Choudekar, D. Asija, and P. V. Astick, "Congestion management of transmission line using smart wire & TCSC with their economic feasibility," in *Computing, Communication and Networking Technologies (ICCCNT), 2017 8th International Conference on*, 2017, pp. 1-5: IEEE.

[8] H. Daneshi and A. Srivastava, "Security-constrained unit commitment with wind generation and compressed air energy storage," *IET Generation, Transmission & Distribution,* vol. 6, no. 2, pp. 167-175, 2012.

[9] P. V. Astick, D. Asija, P. Choudekar, and N. Rani, "Transmission line efficiency enhancement with inclusion of smart wires and controllable network transformers," in *Computing, Communication and Networking Technologies (ICCCNT), 2017 8th International Conference on*, 2017, pp. 1-6: IEEE.

[10] A. Nasri, A. J. Conejo, S. J. Kazempour, and M. Ghandhari, "Minimizing wind power spillage using an OPF with FACTS devices," *IEEE Transactions on Power Systems,* vol. 29, no. 5, pp. 2150-2159, 2014.

[11] ―Smart Wires Press Releases,‖ Smart Wires Inc. [Online]. Available: http://www.smartwires.com/press-releases/.

[12] D. Asija, P. Choudekar, and Y. Manganuri, "Series Smart Wire—Managing Load and Congestion in Transmission Line," in *Proceedings of the 5th International Conference on Frontiers in Intelligent Computing: Theory and Applications*, 2017, pp. 99-107: Springer.

[13] Y. Sang, M. Sahraei-Ardakani, and M. Parvania, "Stochastic Transmission Impedance Control for Enhanced Wind Energy Integration," *IEEE Transactions on Sustainable Energy,* 2017.

[14] O. Ziaee and F. Choobineh, "Stochastic location-allocation of TCSC devices on a power system with large scale wind generation," in *Power and Energy Society General Meeting (PESGM), 2016*, 2016, pp. 1-5: IEEE.

[15] M. Aien, A. Hajebrahimi, and M. Fotuhi-Firuzabad, "A comprehensive review on uncertainty modeling techniques in power system studies," *Renewable and Sustainable Energy Reviews,* vol. 57, pp. 1077-1089, 2016.

[16] D. Bertsimas, E. Litvinov, X. A. Sun, J. Zhao, and T. Zheng, "Adaptive robust optimization for the security constrained unit commitment problem," *IEEE Transactions on Power Systems,* vol. 28, no. 1, pp. 52-63, 2013.

[17] Y. Zhang, N. Gatsis, and G. B. Giannakis, "Robust energy management for microgrids with high-penetration renewables," *IEEE Transactions on Sustainable Energy,* vol. 4, no. 4, pp. 944-953, 2013.

[18] O. Ziaee and F. Choobineh, "Optimal location-allocation of TCSCs and transmission switch placement under high penetration of wind power," *IEEE Transactions on Power Systems,* vol. 32, no. 4, pp. 3006-3014, 2017.

[19] M. Sahraei-Ardakani and K. W. Hedman, "Day-ahead corrective adjustment of FACTS reactance: A linear programming approach," *IEEE Transactions on Power Systems,* vol. 31, no. 4, pp. 2867-2875, 2016.

[20] O. Ziaee, O. Alizadeh-Mousavi, and F. F. Choobineh, "Co-optimization of transmission expansion planning and TCSC placement considering the correlation between wind and demand scenarios," *IEEE Transactions on Power Systems,* vol. 33, no. 1, pp. 206-215, 2018.

[21] S. Dehghan, N. Amjady, and A. J. Conejo, "A Multi-Stage Robust Transmission Expansion Planning Model Based on Mixed-Binary Linear Decision Rules? Part II," *IEEE Transactions on Power Systems,* 2018.

[22] R. T. Force, "The IEEE reliability test system-1996," *IEEE Trans. Power Syst,* vol. 14, no. 3, pp. 1010-1020, 1999.

[23] L. Baringo and A. Conejo, "Correlated wind-power production and electric load scenarios for investment decisions," *Applied energy,* vol. 101, pp. 475-482, 2013.

[24] National Renewable Energy Laboratory (NERL). Wind integration datasets. [Online]. Available: http://www.nrel.gov/grid/wind-integrationdata.html/.

[25] GAMS. The Solver Manuals. 1996 [Online]. Available: http://www.gams.com/.

Ahmad Nikoobakht was born in Iran in 1988. He received the B.Sc. degree in electrical engineering from Hormozgan University, Iran, in 2011, and the M.Sc. and Ph.D. degrees from Shiraz University of Technology, Shiraz, Iran, in 2013 and 2017, respectively. He is currently an Assistance Professor in the Electrical Engineering Department of Higher Education Center of Eghlid, Eghlid, Iran. His research interests include renewable energy systems, smart grids, electricity markets, electric vehicle, demand response, energy storage systems, FACTS devices and optimal planning and operation of power systems, as well as statistics and optimization theory and its applications.

Jamshid Aghaei (M'12-SM'15) received the B.Sc. degree in electrical engineering from the Power and Water Institute of Technology, Tehran, Iran, and the M.Sc. and Ph.D. degrees from the Iran University of Science and Technology, Tehran, Iran, in 2003, 2005, and 2009, respectively. He is currently an Associate Professor with the Shiraz University of Technology, Shiraz, Iran, and a Research Fellow with the Norwegian University of Science and Technology, Trondheim, Norway. His research interests include renewable energy systems, smart grids, electricity markets, and power system operation, optimization, and planning. He is a member of the Iranian Association of Electrical and Electronic Engineers.

Dr. Aghaei is a Subject Editor for the IET Generation Transmission and Distribution, an Associate Editor for the IET Renewable Power Generation. He was the Guest Editor-for the Special Section on ''Industrial and Commercial Demand Response'' of the IEEE Transactions on Industrial Informatics.

Taher Niknam (M'14) received the B.Sc. degree from Shiraz University, Shiraz, Iran, and the M.Sc. and Ph.D. degrees from Sharif University of Technology, Tehran, Iran, in 1998, 2000, and 2005, respectively, all in power electrical engineering. He is currently a Full Professor with Shiraz University of Technology, Shiraz, Iran. His research interests include power system restructuring, impacts of distributed generations on power systems, optimization methods, and evolutionary algorithms.

This article has been accepted for publication in a future issue of this journal, but has not been fully edited. Content may change prior to final publication. Citation information: DOI 10.1109/TSTE.2018.2877106, IEEE Transactions on Sustainable Energy

Miadreza Shafie-khah (M'13-SM'17) received the M.Sc. and Ph.D. degrees in electrical engineering from Tarbiat Modares University, Tehran, Iran, in 2008 and 2012, respectively. He received his first postdoc from the University of Beira Interior (UBI), Covilha, Portugal in 2015, while working on the 5.2-million-euro FP7 project SiNGULAR ("Smart and Sustainable Insular Electricity Grids Under Large-Scale Renewable Integration"). He received his second postdoc from the University of Salerno, Salerno, Italy in 2016. He was an Assistant Professor eq. (Visiting Scientist) at C-MAST/UBI. Currently, he is an Assistant/Senior Researcher at INESC TEC. He was considered one of the Outstanding Reviewers of the IEEE TRANSACTIONS ON SUSTAINABLE ENERGY, in 2014 and 2017, one of the Best Reviewers of the IEEE TRANSACTIONS ON SMART GRID, in 2016 and 2017, and one of the Outstanding Reviewers of the IEEE TRANSACTIONS ON POWER SYSTEMS, in 2017. His research interests include power market simulation, market power monitoring, power system optimization, demand response, electric vehicles, price forecasting and smart grids.

João P. S. Catalão (M'04-SM'12) received the M.Sc. degree from the Instituto Superior Técnico (IST), Lisbon, Portugal, in 2003, and the Ph.D. degree and Habilitation for Full Professor ("Agregação") from the University of Beira Interior (UBI), Covilha, Portugal, in 2007 and 2013, respectively.

Currently, he is a Professor at the Faculty of Engineering of the University of Porto (FEUP), Porto, Portugal, and Researcher at INESC TEC, INESC-ID/IST-UL, and C-MAST/UBI. He was also appointed as Visiting Professor by North China Electric Power University, Beijing, China. He was the Primary Coordinator of the EU-funded FP7 project SiNGULAR ("Smart and Sustainable Insular Electricity Grids Under Large-Scale Renewable Integration"), a 5.2-million-euro project involving 11 industry partners. He has authored or coauthored more than 675 publications, including 252 journal papers (more than 75 IEEE Transactions/Journal papers), 370 conference proceedings papers, 5 books, 34 book chapters, and 14 technical reports, with an *h*-index of 43, an *i10*-index of 173, and over 7380 citations (according to Google Scholar), having supervised more than 70 post-docs, Ph.D. and M.Sc. students. He is the Editor of the books entitled *"Electric Power Systems: Advanced Forecasting Techniques and Optimal Generation Scheduling"* and *"Smart and Sustainable Power Systems: Operations, Planning and Economics of Insular Electricity Grids"* (Boca Raton, FL, USA: CRC Press, 2012 and 2015, respectively). His research interests include power system operations and planning, hydro and thermal scheduling, wind and price forecasting, distributed renewable generation, demand response and smart grids.

Prof. Catalão is an Editor of the IEEE TRANSACTIONS ON SMART GRID, an Editor of the IEEE TRANSACTIONS ON POWER SYSTEMS, an Associate Editor of the IEEE TRANSACTIONS ON INDUSTRIAL INFORMATICS, and a Subject Editor of the *IET Renewable Power Generation*. From 2011 till 2018 (seven years) he was an Editor of the IEEE TRANSACTIONS ON SUSTAINABLE ENERGY and an Associate Editor of the *IET Renewable Power Generation*. He was the Guest Editor-in-Chief for the Special Section on "Real-Time Demand Response" of the IEEE TRANSACTIONS ON SMART GRID, published in December 2012, the Guest Editor-in-Chief for the Special Section on "Reserve and Flexibility for Handling Variability and Uncertainty of Renewable Generation" of the IEEE TRANSACTIONS ON SUSTAINABLE ENERGY, published in April 2016, and the Corresponding Guest Editor for the Special Section on "Industrial and Commercial Demand Response" of the IEEE TRANSACTIONS ON INDUSTRIAL INFORMATICS, to be published in November 2018. Since March 2018, he is the Lead Guest Editor for the Special Issue on "Demand Side Management and Market Design for Renewable Energy Support and Integration" of the *IET Renewable Power Generation*. He was the recipient of the 2011 Scientific Merit Award UBI-FE/Santander Universities, the 2012 Scientific Award UTL/Santander Totta, the 2016 FEUP Diploma of Scientific Recognition, and the Best INESC-ID Researcher 2017 Award, in addition to an Honorable Mention in the 2017 Scientific Awards ULisboa/Santander Universities. Moreover, he has won 4 Best Paper Awards at IEEE Conferences.